The Effect of Airbag Design on Impact Attenuation for Hip Protection

Thanaphon Hongsakun
Department of Mechanical Engineering, Faculty of Engineering, Prince of Songkla University, Thailand
thanaponhongsakul@gmail.com

Boonsin Tangtrakulwanich
Department of Orthopedics, Faculty of Medicine, Prince of Songkla University, Thailand
boonsin.b@psu.ac.th

Nitipan Vittayaphadung
Department of Mechanical Engineering, Faculty of Engineering, Prince of Songkla University, Thailand
nitipan.v@psu.ac.th

Wiriya Thongruang
Department of Mechanical Engineering, Faculty of Engineering, Prince of Songkla University, Thailand
wiriya.t@psu.ac.th

Satta Srewaradachpisal
Department of Mechanical Engineering, Faculty of Engineering, Prince of Songkla University, Thailand | Smart Industry Research Center, Department of Industrial and Manufacturing Engineering, Faculty of Engineering, Prince of Songkla University, Thailand
satta.s@psu.ac.th (corresponding author)

Received: 12 March 2025 | Revised: 18 April 2025 and 7 May 2025 | Accepted: 10 May 2025

 DOI: https://doi.org/10.48084/etasr.10907

ABSTRACT

This study examines the impact attenuation performance of airbags of different shapes, thicknesses, and internal pressures to assess their effectiveness in hip protection. Three distinct airbag shapes are examined and analyzed under different thicknesses and pressures, with experimental tests conducted to assess the relationships between thickness, pressure, stiffness, and impact absorption efficiency. The results reveal that increasing the thickness of the airbag significantly reduces the peak impact force, while higher internal pressure increases stiffness but does not always lead to improveð impact attenuation. Among the three airbag shapes, the torus-shaped airbag demonstrates the lowest peak impact force and the highest impact absorption efficiency. Additionally, airbags maintained at atmospheric pressure (0 psi) exhibit the greatest impact absorption efficiency, followed by those at 3 psi and 6 psi, respectively. Comparing existing studies on traditional hip protectors, the results indicate that airbags provide a superior reduction in impact force. Unlike conventional hip protectors, which primarily rely on direct force absorption, the torus airbag employs an off-loading mechanism to dissipate impact energy, thereby enhancing its protective performance. These findings suggest that airbag-based protective systems could serve as an innovative solution for reducing fall-related injuries.

Keywords-fall; hip fracture; airbag; impact force

I. INTRODUCTION

Osteoporosis is more common in older individuals and can affect various parts of the body, such as the jawbone [1], hip, and other skeletal regions. Older adults with osteoporosis are at a significantly higher risk of hip fractures due to falls. Public health data indicate that falls are prevalent among the elderly, often resulting in severe injuries and even fatalities [2]. Hip fractures in older adults are a major contributor to morbidity and mortality. Studies have shown that the lifetime risk of sustaining a hip fracture is 23.3% in women and 11.2% in men [3]. The average life expectancy after experiencing a hip fracture is approximately six years [4], with a one-year mortality rate reaching up to 26% [5], and the highest risk

occurring within the first six months. Moreover, patients who survive hip fractures often suffer from chronic pain for one to two years post-fracture [6]. Only 40% of patients regain independent ambulation one year after the injury [7]. Currently, there are three methods for preventing hip fractures from falls: Compliant Flooring, designed to absorb impact in the case of a fall and reduce the force exerted on the hips or head by up to 50%. However, trials in elderly care facilities have shown that it has not yet clearly reduced injury rates. Experiments in long-term care facilities have found that, although this type of flooring does not increase fall rate, it does not significantly reduce injury rate in long-term care [8]. Passive Wearables, such as hip protectors, use cushioning materials to help absorb the impact force in the case of a fall. Their primary advantages are low cost and ease of production. However, there are challenges with their acceptance among the elderly due to discomfort and inconsistent use. Moreover, research indicates that adherence to recommendations for wearing hip protectors often decreases over time, which is a significant issue for the long-term use of passive protective devices [9]. Active wearables, such as belts with airbags, are equipped with falling detection sensors. When a fall is detected, the system rapidly inflates the airbags to protect the hips before impact. Authors in [10] conducted a study in a long-term care setting, demonstrating that an active smartbelt system with automated airbag deployment successfully reduced the force of hip impact during falls. The study also showed high adherence among elderly users, addressing a common limitation seen in passive hip protectors. This indicates that active wearable devices not only offer superior impact mitigation but are also more likely to be consistently used in daily life, making them a promising solution for fall-related hip fracture prevention in older adults. Additionally, laboratory studies suggest that these devices have the potential to significantly reduce impact force during falls [11]. Authors in [12] investigated impact reduction using six types of hip pads and airbags, with experiments being conducted on a hip impact simulator. The results indicate that airbags significantly outperform conventional hip pads in absorbing impact forces, suggesting that emerging wearable technologies could play a crucial role in preventing hip fractures in high-risk populations.

Airbags are modern hip protection devices that offer higher protective efficiency compared to hip pads. Studies on the structure of hip protection belts with airbags identify three main components: sensors, a gas inflation mechanism, and the airbag. Historically, researchers have primarily focused on sensor-related studies. Previous studies [13-15] have explored the development of fall detection algorithms using acceleration and angular velocity signals, along with testing airbag systems that employ gunpowder for rapid inflation. The design and development of fall detection algorithms utilizing various sensors and spring-trigger mechanisms that release cold gas to inflate airbags is then proposed by studies [16-17], which found that these methods are safer and more portable than gunpowder. Those general sensors are MEMS-based IMU sensors and three-axis accelerometers (MPU-6050 modules). Further studies [18-20] introduced wearable sensor-based systems for fall detection with notification systems. While some focused on activity recognition using deep learning algorithms [18], others implemented real-time alert mechanisms to notify caregivers via SMS, with certain systems also integrating airbag deployment for enhanced protection [19-20].

While these works have advanced fall detection technologies and inflation mechanisms, limited attention has been given to the design parameters of the airbags themselves, such as shape, thickness, and internal pressure—factors that are directly related to impact attenuation. Although some studies have reported airbag sizes, such as 250 × 450 mm with a 10-liter gas capacity [13] or 900 × 260 × 75 mm with a 12-liter capacity [17], there is little discussion about the rationale behind these dimensions. Several studies did not specify the size or shape of the airbags at all, relying solely on images [16, 19-20]. Most existing research has employed rectangular airbags without justification for their design choices. In addition, the impact absorption performance of these airbags is often not empirically validated, raising concerns that improperly designed airbags may fail to prevent serious injury. While authors in [12] conducted impact force testing, the study was limited to a single airbag design, lacking variation in airbag shape or configuration. These limitations highlight a significant knowledge gap in the current literature regarding how airbag shape, size, and internal pressure interact to influence mechanical response and impact attenuation.

Therefore, the current study aims to investigate the key design parameters of hip-protection airbags using a hip impact simulator. The parameters under investigation include shape (cubic, cylindrical, toroidal), thickness (50, 70, 90 mm), and internal pressure (0, 3, 6 psi). To the best of the authors' knowledge, previous studies have not simultaneously analyzed these three variables in the context of hip-protection airbag design. Exploring these parameters will help fill the knowledge gap related to airbag design for hip protection. The findings from this study are expected to benefit researchers, developers, and manufacturers in advancing more effective airbag-based systems for hip fracture prevention in the future.

II. MATERIALS AND METHODS

The airbags used in this study are made from 100% nylon fabric coated with Polyurethane (PU) to make them both water-repellent (W/R) and waterproof (W/P), with a thickness of 0.1 mm. The airbags are stitched with two layers and shaped into three forms: cubic, cylindrical, and torus; each shape maintains a constant cross-section with an approximate surface area of 38,000 mm², as illustrated in Figure 1(a). Each shape has a thickness of 50, 70, and 90 mm, as shown in Figure 1(b), identified in this study as T50, T70, and T90, respectively, culminating in a total of nine airbag samples. After stitching, the seams are coated with an acrylic resin adhesive combined with a hardening agent. The same type of fabric is then attached along the seams. The airbag is then connected to a PU air hose with an Outer Diameter (OD) of 8 mm and an Inner Diameter (ID) of 5 mm.

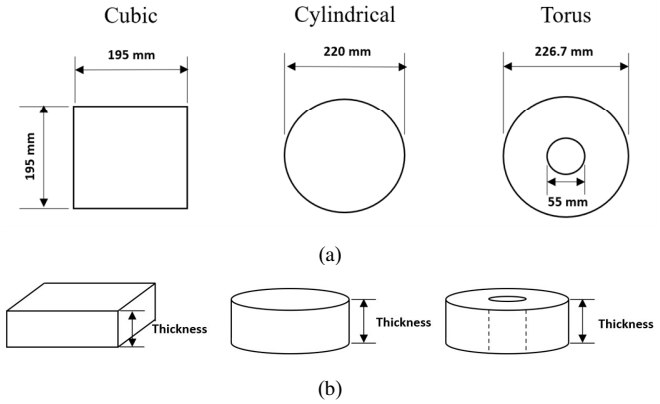

Fig. 1. (a) Airbag dimensions by shape, (b) thickness, or (c) top and bottom distance.

A. Physical Properties

The physical properties examined in this study included the increased volume and dimension (thickness and width) only before impact testing of the airbags under each pressure condition. Dimensional Measurement: The height and width of the airbags were measured at 0, 3, and 6 psi using a Vernier Height Gage to quantify the changes in their physical dimensions under increasing internal pressure. Volume Measurement: The airbags were inflated to pressures of 0, 3, and 6 psi using a pressure gauge (scale: 0–14 psi, resolution: 0.2 psi). Each airbag was then submerged in a water-filled container, displacing a measurable amount of water. The displaced water volume was recorded to determine the total airbag volume at each pressure level. The data obtained from these measurements are summarized in Tables I and II, which present the variations in dimensions and volume across different airbag shapes and pressure levels.

B. Mechanical Testing

In this study, mechanical testing of the airbags under each condition was conducted to evaluate stiffness using a compression method. A universal testing machine (Model Instron 8872), illustrated in Figure 2, was used to determine the relationship between compressive force and airbag displacement in each condition at a compression speed of 100 mm/min. The tests were conducted within a force range of 0 to 1000 N. The equations for the force-displacement relationship of each airbag were derived using SigmaPlot software. The equations were subsequently employed to determine the stiffness [21]. Each airbag was tested at three different pressures: 0, 3, and 6 psi, with a total of 27 experiments conducted.

C. Drop Testing Apparatus

Figure 3 displays the construction of the testing apparatus designed to simulate the impact forces on the femoral bone in compliance with the specific published research [22, 23] and the Canadian standard (CSA). This setup employed a test mass of 28 kg, which was chosen based on biomechanical studies to approximate the effective mass of the pelvis during a sideways fall (22–33 kg). Studies have shown that approximately 25–35% of total body mass contributes directly to the impact at the greater trochanter during sideways falls [23]. The system included a spring with a stiffness of 47 kN/m and a length of 370 mm. The impact plate measured 200 mm in diameter, differing from the standard since the original design was intended for smaller hip pads rather than the airbags tested here. Therefore, the researchers adjusted the size to better accommodate the airbags.

Fig. 2. Compression testing of airbags.

The mass was held by an electromagnet before being released for testing. The hip model was cast from aluminum, with the force on the hip model measured by a load cell (Kistler type 9321B Fz max ±10 kN). The tissue layer was composed of RA-325 silicone mixed with a silicone accelerator at a ratio of 1.5%-2% of the silicone weight, and the impact area was designed to have a thickness of 24 mm.

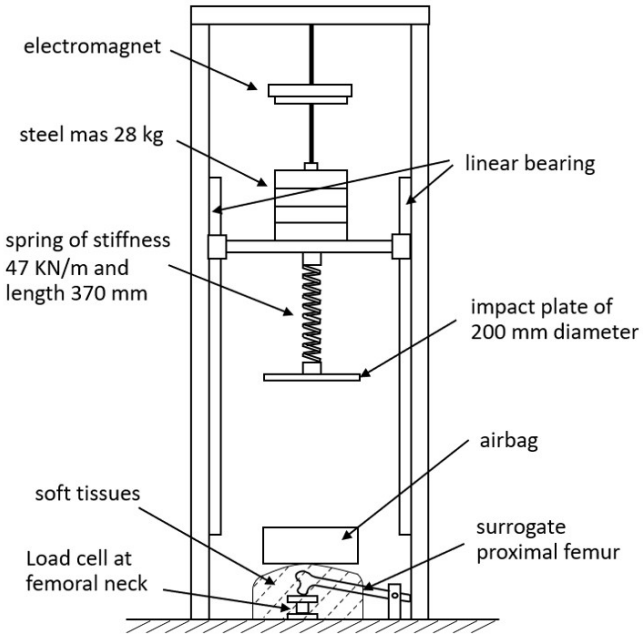

Fig. 3. Drop tower test set.

In this experiment, a steel mass was dropped from a height of 460 mm onto the tissue to measure the impact force in an unpadded condition. The drop height was determined based on the impact velocity used in the experiment, which was set at 3 m/s, following the findings of [23], where the average impact velocity of the hip was reported as 3.01 m/s. This resulted in an impact energy of 126 J, which aligns with the reported impact energy range of 100–200 J in actual falls [23]. Following this, the airbag was placed on the tissue to evaluate the impact force, with a low impact force indicating effective reduction by the airbag. Each airbag was tested at three different pressures: 0, 3, and 6 psi, with each test repeated three times, resulting in a total of 81 trials.

III. RESULTS AND DISCUSSIONS

A. *Physical Properties*

This section focuses on examining two key aspects of the airbags' physical properties: size and volume, as portrayed in Figure 4. Specifically, the Percentage Change in Airbag Dimensions (PCAD), including thickness, width, and volume was calculated using:

$$PCAD = \frac{Original\ dimension - Final\ dimension}{Original\ dimension} \times 100 \quad (1)$$

The results indicate that an increase in airbag pressure leads to a corresponding increase in the percentage change for both thickness and width, as demonstrated in Table I. However, the increase in thickness was notably more pronounced compared to the change in width, which remained relatively marginal.

Regarding the percentage increase in thickness, the cubic airbag exhibited a substantial increase, ranging from approximately 54% to 122%, while the cylindrical airbag exhibited an increase of approximately 47% to 112%. In contrast, the torus airbag displayed a relatively modest increase in thickness, ranging from approximately 12% to 30%. Conversely, the percentage increase in width was markedly lower across all airbag shapes. The cubic airbag showed a width increase of approximately 0%-6%, the cylindrical airbag an increase of approximately 0%-5%, and the torus airbag an increase of only 0%-1%.

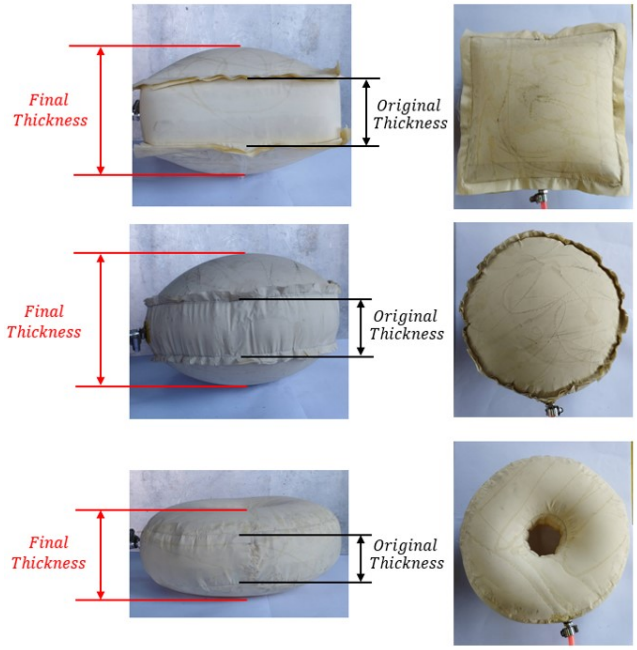

Fig. 4. Airbag expansion.

The findings suggest that an increase in thickness has a more significant impact on airbag expansion compared to an increase in width. This discrepancy can be attributed to the reduced constraint on expansion along the top and bottom surfaces of the airbags, allowing for greater deformation, while the expansion along the sides was more restricted. Consequently, the airbags predominantly expanded in the thickness direction. This behavior aligns with previous research indicating that cylindrical shapes exhibit greater resistance to internal pressure compared to cubic shapes [24-26]. As emphasized in [27], the superior pressure resistance of cylindrical structures tends to be consistent with their fundamental geometric and structural characteristics. However, this study reveals that the torus-shaped airbag exhibited even better pressure resistance than the cylindrical design.

The percentage change in airbag volume relative to the initial volume is presented in Table II .The data indicate that as pressure increases, the percentage of volume expansion also increases. Specifically, the cubic airbag exhibits a volume increase of approximately 40%-140%, the cylindrical airbag shows an increase of approximately 22%-113%, and the torus airbag demonstrates a more modest increase of approximately 22%-73%. These observed changes in volume are attributed to alterations in both thickness and width.

TABLE I. CHANGES IN THICKNESS AND WIDTH DIMENSIONS OF THE AIRBAGS UNDER PRESSURE

Airbag	0 psi				3 psi				6 psi			
	Thickness		Width		Thickness		Width		Thickness		Width	
	(mm)	(%)	(mm)	(%)	(mm)	(%)	(mm)	(%)	(mm)	(%)	(mm)	(%)
Cubic T50	98	96.00	195	0.00	105	110.00	197	1.02	111	122.00	200	2.56
Cubic T70	119	70.00	200	2.56	124	77.14	205	5.12	132	88.57	208	6.66
Cubic T90	139	54.44	201	3.07	146	62.22	205	5.12	155	72.22	208	6.66
Cylindrical T50	93	86.00	220	0.00	99	98.00	224	1.81	106	112.00	227	3.18
Cylindrical T70	114	62.85	221	0.45	121	72.85	227	3.18	133	90.00	230	4.54
Cylindrical T90	133	47.77	223	1.36	141	56.66	227	3.18	148	64.44	232	5.45
Torus T50	60	20.00	228	0.57	63	26.00	229	1.01	65	30.00	229	1.01
Torus T70	81	15.71	228	0.57	84	20.00	229	1.01	85	21.42	230	1.45
Torus T90	101	12.22	229	1.01	104	15.55	229	1.01	106	17.77	230	1.45

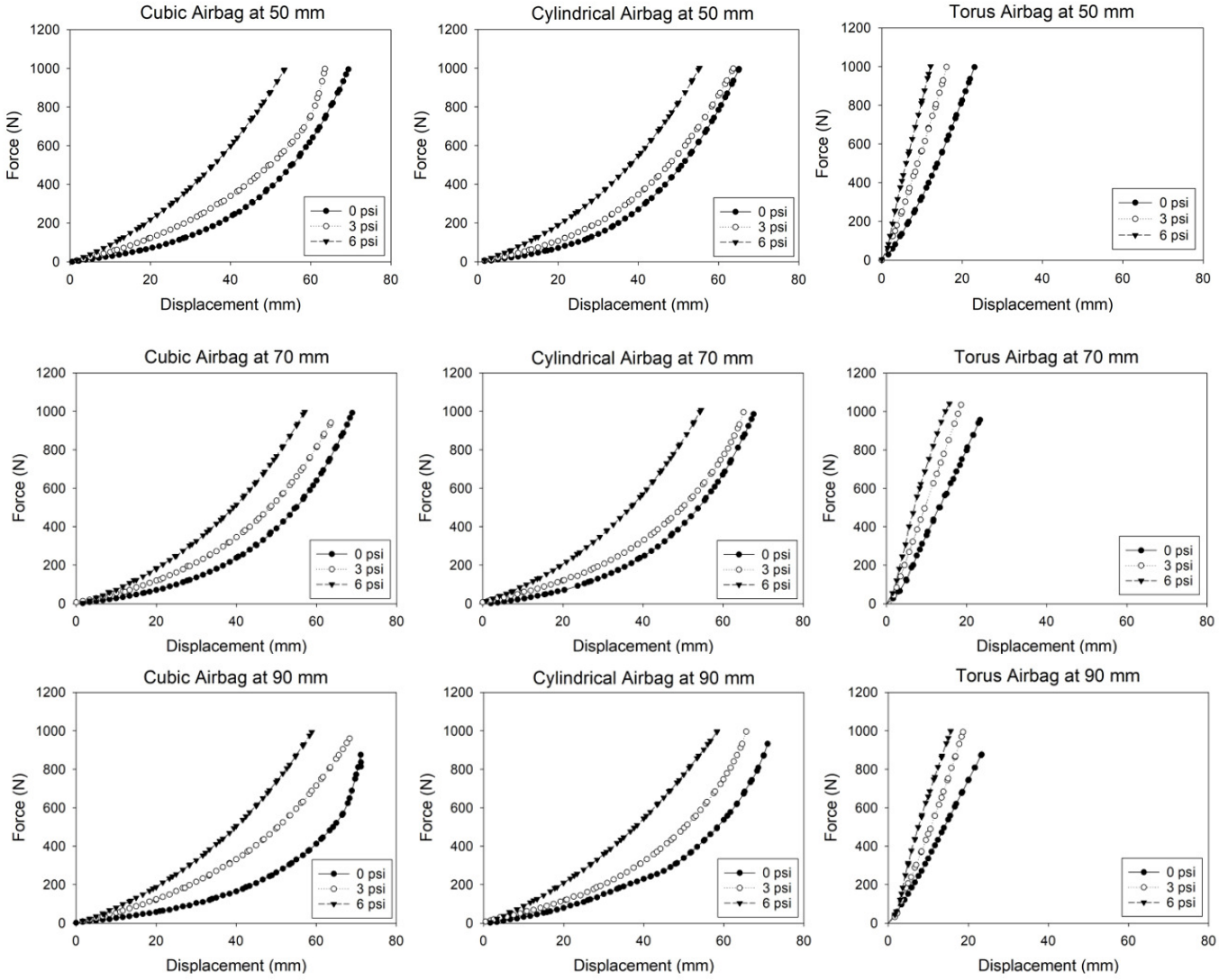

Fig. 5. Graphs of the relationship between force and displacement.

As pressure increases, both dimensions expand, resulting in a corresponding increase in airbag volume. However, when the thickness of the airbag increases, the percentage change in volume decreases. This trend is consistent with the reduced percentage change in thickness observed under these conditions. The primary reason for this behavior is that changes in width are considerably smaller compared to changes in thickness, thereby limiting the overall extent of volume expansion.

TABLE II. PERCENTAGE VOLUME INCREASE FROM THE AIRBAG DESIGN UNDER PRESSURE

Airbag	0 psi (%)	3 psi (%)	6 psi (%)
Cubic T50	86.76	106.77	140.13
Cubic T70	42.93	61.99	81.05
Cubic T90	40.81	66.75	85.28
Cylindrical T50	80.24	100.27	113.62
Cylindrical T70	52.58	71.66	81.19
Cylindrical T90	22.38	33.51	48.34
Torus T50	46.96	53.64	73.68
Torus T70	24.06	33.60	52.68
Torus T90	22.46	33.60	48.44

B. Stiffness Properties

Figure 5 displays the results of the mechanical property tests, illustrating the correlation between force and airbag deflation distance. A comparison of different pressure levels indicates that higher pressures yield steeper slopes, reflecting a greater rate of force increase for the same displacement. Furthermore, when comparing airbags of varying thicknesses, it was observed that greater thickness results in a reduced slope of the graph. These results are consistent with those of previous studies [21, 28], where it was suggested that increasing the air mass within the airbag (or increasing the pressure) leads to greater force and stiffness while maintaining constant displacement. Additionally, it is evident that the graph for the torus airbag exhibits a linear trend, whereas the graphs for the cubic and cylindrical airbags display a curved pattern.

The mechanical properties of the airbags are illustrated through two types of graphs: linear and curved. These relationships can be mathematically expressed using curve fitting under a polynomial equation format, as demonstrated in:

$$y = y_0 + ax + bx^2 + cx^3 \quad (2)$$

The torus airbag adheres to a linear equation, representing a first-degree, while the cubic and cylindrical airbags, characterized by curved graphs, correspond to higher-degree polynomial equations. By differentiating these equations once, the stiffness equations are derived. The torus airbag yields a constant stiffness value, whereas the cubic and cylindrical airbags produce equations that require substituting x (displacement) to determine stiffness. The value of x is calculated as the difference between the initial thickness (such as 50 mm for airbag T50, as presented in Table I) and the deflection distance between the top and bottom edges. Stiffness values are also visually represented in Figure 6, providing a comparative perspective on the structural behavior of different airbag designs.

As shown in Figure 6, all three graphs exhibit a similar pattern: Stiffness decreases as thickness increases and rises with an increase in pressure. In addition, it can be seen that the torus airbag has the highest stiffness, while the cubic and cylindrical airbags have similar stiffness values, with the cubic airbag being slightly higher than the cylindrical one. This is consistent with [29], where the findings reveal that the stiffness of an airbag depends on the initial internal pressure and the geometric shape of the airbag.

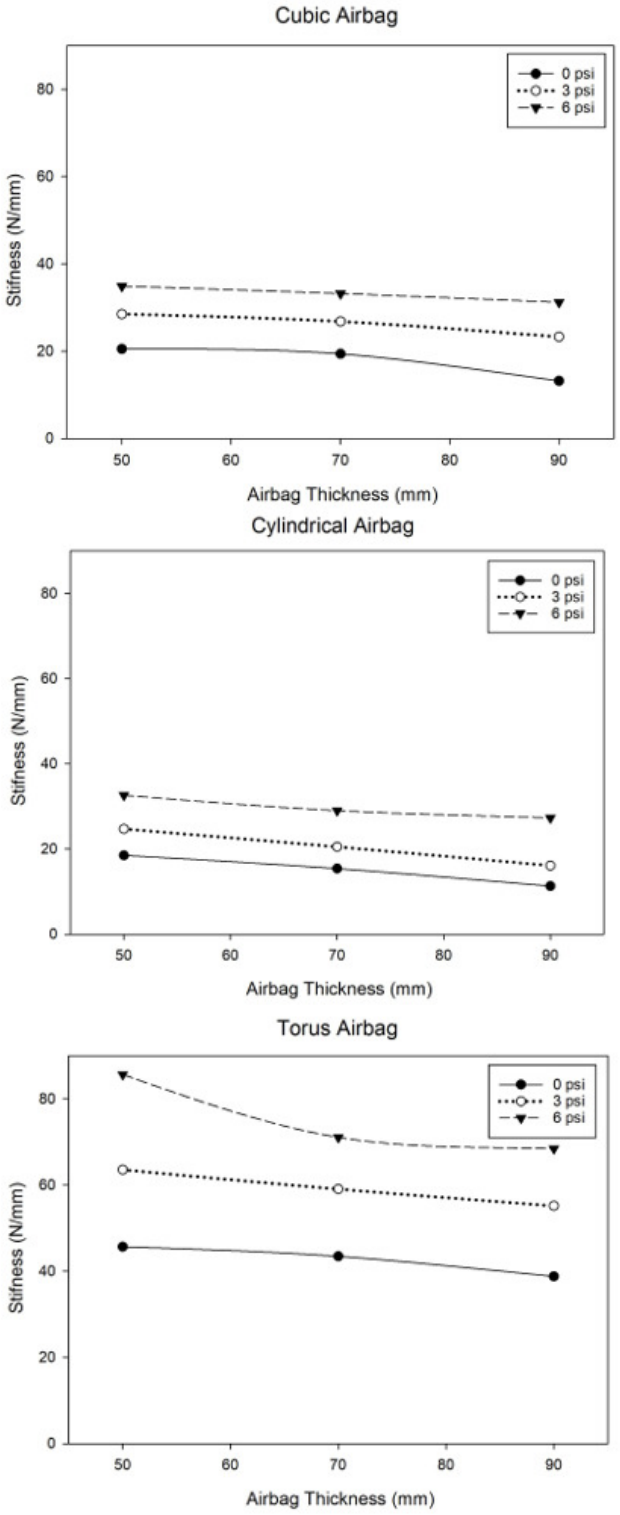

Fig. 6. Graph of the relationship between stiffness and thickness of a cubic airbag, a cylindrical airbag, and a torus airbag.

C. Impact Forces Testing

According to the drop testing apparatus and mechanical testing, the airbags were able to withstand the load without

damage and could be reused for repeated tests. The airbags can be seen in Figure 7. Figure 8 illustrates the relationship between force and airbag thickness. The graph reveals a consistent trend across all three airbag types: An increase in thickness results in a reduction of peak impact force. This finding is consistent with those in [30], where the effect of thickness on impact force attenuation was investigated using Shear-Thickening Polymer (STP) hip protectors ranging from 4 mm to 12 mm. The results indicated that as the thickness of the hip protector (STP) increased, the force transmitted to the hip decreased.

Conversely, increasing the internal pressure of the airbag also results in a peak impact force reduction. This observation aligns with the stiffness values presented in Figure 6, where an increase in thickness corresponds to a decrease in stiffness, while an increase in pressure leads to higher stiffness and greater force generation. Although the study in [29] agrees with this study/the present study in that the initial pressure of the airbag influences its stiffness, it contradicts this work by suggesting that internal pressure has a minimal direct effect on reducing the impact force. This discrepancy may be due to the relatively narrow pressure range (0–2500 Pa) examined in that study. In contrast, this study demonstrates that pressure significantly contributes to the reduction in impact force.

When comparing different airbag shapes, the torus airbag exhibited the lowest peak impact force, followed by the cylindrical and cubic airbags, respectively.

(a) (a) (a)

Fig. 7. (a) Cubic airbag, (b) cylindrical airbag, and (c) torus airbag.

This indicates that shape significantly influences energy absorption capabilities. The cubic airbag experienced the highest impact force, with the cylindrical airbag showing similar but slightly lower values. The effect of shape is closely related to the contact area. In studies involving hip protectors, all three designs had identical surface sizes, resulting in comparable contact areas. This is consistent with the simulations of various hip protector designs, which reported similar findings [12]. Perforated hip protectors were found to provide superior impact force reduction across all thicknesses and surface areas, which is consistent with [31], where a design approach is descrived, involving 'forming a bridge over the trochanter to shunt the energy of the fall to surrounding regions, where it can be absorbed more safely' [23]. However, such a design requires careful consideration of the force distribution points to maximize impact reduction efficiency [32].

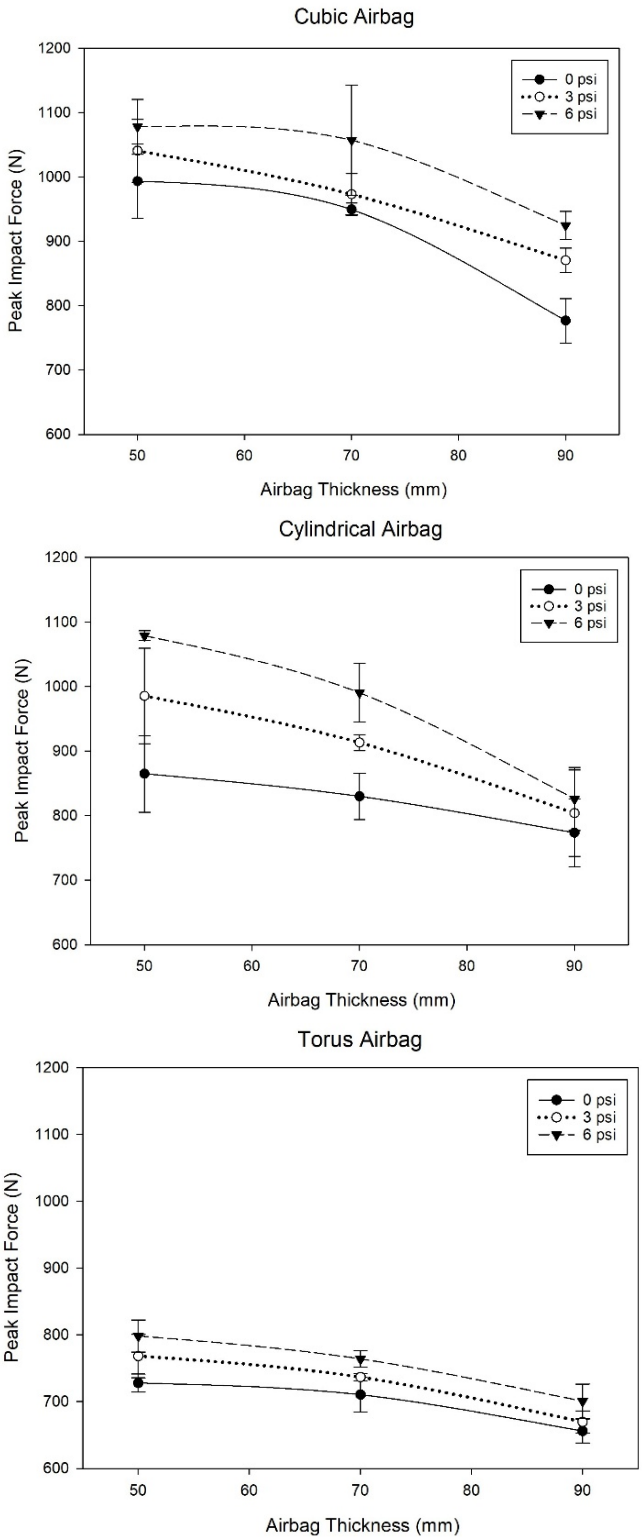

Fig. 8. Graph of the relationship between force and thickness of a cubic airbag, a cylindrical airbag, and a torus airbag.

The torus airbag, despite having the highest stiffness, exhibited the lowest impact force. This contradicts the

assumption that impact force is directly proportional to stiffness, as the torus airbag dissipates impact forces through an off-loading mechanism rather than direct absorption, unlike the cubic and cylindrical airbags. This is consistent with [33], where perforated and non-perforated hip protectors were compared. It was found that perforated hip protectors reduced impact force by approximately 30%-50% compared to non-perforated ones. The presence of perforations helps distribute the impact force more effectively rather than concentrating directly on the bone.

The results of all impact force tests showed that the condition with the highest impact force was the cubic airbag, with a thickness of 50 mm at 6 psi (1,077.97 ± 42.45 N). Conversely, the condition with the lowest mean impact force was the torus airbag, with a thickness of 90 mm at 0 psi (655.91 ± 17.85 N).

D. Impact Absorption Efficiency or Cushioning Properties

The value of impact absorption capability represents the ability to reduce the impact force experienced by the hip bone compared to the case without an airbag. For the unpadded condition, the mean impact force was 2,834.66 ± 20.13 N. The calculation was performed using:

$$Percent\ Impact\ absorption = \frac{unpadded - Force}{unpadded} \times 100 \quad (3)$$

The impact absorption properties of the different airbags are shown in Figure 9.

According to Figure 9, the impact absorption efficiency of all three airbag shapes increases exponentially with greater thickness. Across all conditions, the thickness of 90 mm provided the highest impact absorption efficiency, followed by 70 mm and 50 mm, respectively. Additionally, the impact absorption efficiency of all three airbag shapes decreased as pressure increased. In all cases, the pressure level yielding the highest impact absorption efficiency was 0 psi (atmospheric pressure), followed by 3 psi and 6 psi, respectively. Furthermore, among the airbag shapes, the torus airbag exhibited the highest impact absorption efficiency, ranging from 71.83% to 75.28%, followed by the cylindrical airbag, ranging from 61.94% to 70.86%. The cubic airbag demonstrated the lowest impact absorption efficiency, ranging from 61.97% to 67.37%.

In comparison to the study in [34], where the effectiveness of three types of hip protectors was tested and it was found that the most effective one reduced impact force by 33.5%, this study revealed airbags to be significantly more effective at absorbing impact forces than traditional hip protectors. This finding is consistent with those in [12], where the effectiveness of six types of hip protectors and an airbag was evaluated, concluding that the airbag had the highest impact absorption efficiency, ranging from 54% to 58%. Notably, this range is relatively similar to the impact absorption efficiency observed for the cylindrical and cubic airbags in this study.

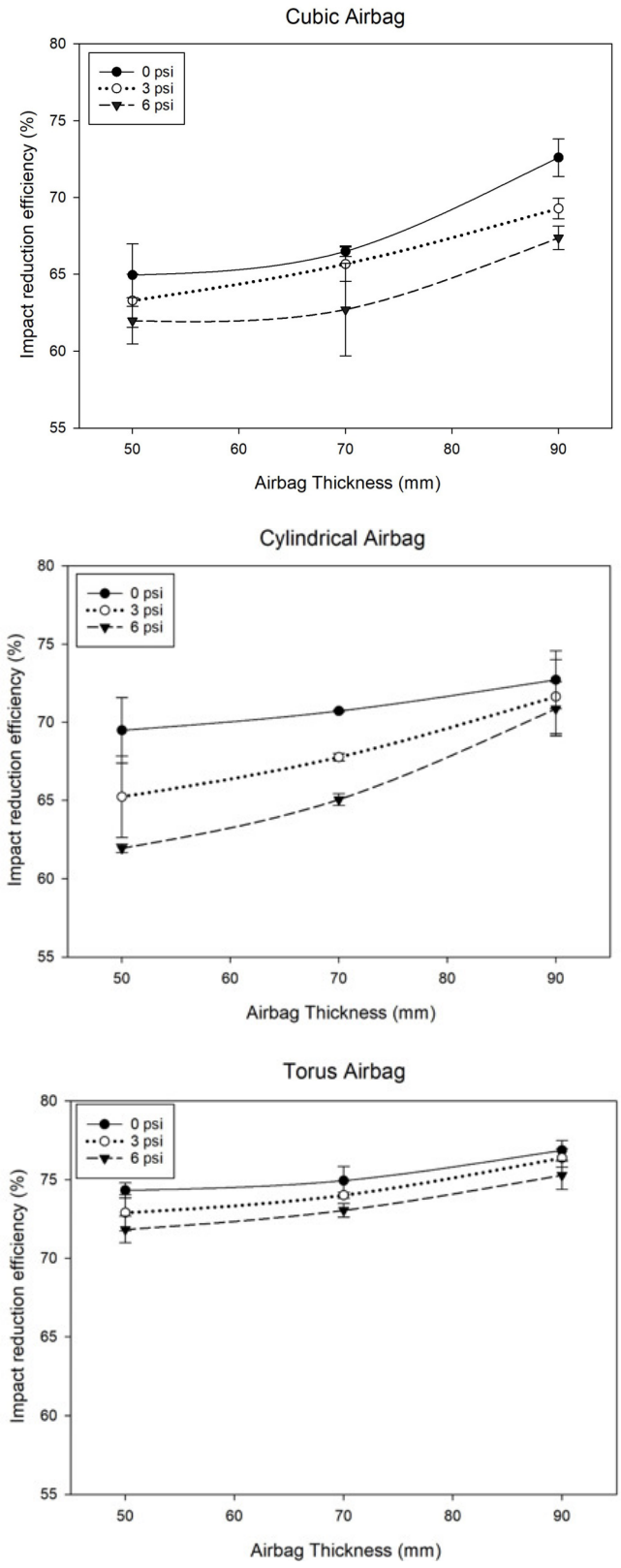

Fig. 9. Graph of the relationship between impact force efficiency and thickness of a cubic airbag, a cylindrical airbag, and a torus airbag.

IV. CONCLUSIONS

This study examined the effects of airbag design on impact attenuation for hip protection by evaluating different airbag shapes, thicknesses, and internal pressures. The results indicate that increasing airbag thickness significantly reduces peak impact force, while higher internal pressure increases stiffness but does not consistently improve impact attenuation. Among the three airbag geometries studied, the torus airbag exhibited the lowest peak impact force, followed by the cylindrical and cubic airbags. This finding underscores the importance of airbag shape in impact absorption efficiency, with the torus design proving to be the most effective. The impact absorption efficiency of all airbags increased with greater thickness, with the 90 mm airbags performing the best, followed by 70 mm and 50 mm, respectively. In contrast, higher internal pressure led to a reduction in impact absorption efficiency, with airbags at 0 psi demonstrating the highest performance, followed by those at 3 psi and 6 psi, respectively. Among the tested shapes, the torus airbag exhibited the highest efficiency (71.83%-75.28%), followed by the cylindrical (61.94%-70.86%) and cubic (61.97%-67.37%) airbags. These findings suggest that optimizing shape and thickness, rather than relying on high internal pressure, is key to achieving superior impact attenuation performance. Comparisons with traditional hip protectors from prior studies further highlight the superior impact attenuation capabilities of airbag-based systems [12], indicating their potential as a more effective solution for preventing fall-related injuries. In contrast to [29], where limited influence of internal pressure was reported, the current study's results show significant pressure effects likely due to a broader testing range. Furthermore, the torus airbag design, with its off-loading mechanism, mirrors the efficiency of perforated protectors discussed in [31, 33], highlighting its superior performance in dissipating impact energy.

Overall, this study offers valuable insights into the role of airbag design in impact mitigation and proposes that future research should explore material composition, deployment mechanisms, and clinical aspects to further advance hip protection technologies.

ACKNOWLEDGMENT

This research was supported by National Science, Research and Innovation Fund (NSRF) and Prince of Songkla University (Ref. No. MED6701005b). The authors would like to thank the Department of Mechanical Engineering, Faculty of Engineering, the Department of Orthopedics, Faculty of Medicine, Prince of Songkla University, Thailand for the provision of the experimental facilities in the research.

REFERENCES

[1] R. F. A. Marar, D. M. Uliyan, and H. A. Al-Sewadi, "Mandible Bone Osteoporosis Detection using Cone-beam Computed Tomography," *Engineering, Technology & Applied Science Research*, vol. 10, no. 4, pp. 6027–6033, Aug. 2020, https://doi.org/10.48084/etasr.3637.

[2] D. Houry, C. Florence, G. Baldwin, J. Stevens, and R. McClure, "The CDC Injury Center's Response to the Growing Public Health Problem of Falls Among Older Adults," *American Journal of Lifestyle Medicine*, vol. 10, no. 1, pp. 74–77, Jan. 2016, https://doi.org/10.1177/1559827615600137.

[3] J. A. Kanis *et al.*, "Long-Term Risk of Osteoporotic Fracture in Malmö," *Osteoporosis International*, vol. 11, no. 8, pp. 669–674, Sep. 2000, https://doi.org/10.1007/s001980070064.

[4] S. R. Cummings and L. J. Melton, "Epidemiology and outcomes of osteoporotic fractures," *The Lancet*, vol. 359, no. 9319, pp. 1761–1767, May 2002, https://doi.org/10.1016/S0140-6736(02)08657-9.

[5] A. Trombetti, F. Herrmann, P. Hoffmeyer, M. A. Schurch, J. P. Bonjour, and R. Rizzoli, "Survival and Potential Years of Life Lost After Hip Fracture in Men and Age-matched Women," *Osteoporosis International*, vol. 13, no. 9, pp. 731–737, Sep. 2002, https://doi.org/10.1007/s001980200100.

[6] J. D. Adachi *et al.*, "The association between osteoporotic fractures and health-related quality of life as measured by the Health Utilities Index in the Canadian Multicentre Osteoporosis Study (CaMos)," *Osteoporosis International*, vol. 14, no. 11, pp. 895–904, Nov. 2003, https://doi.org/10.1007/s00198-003-1483-3.

[7] C. Cooper, "The crippling consequences of fractures and their impact on quality of life," *The American Journal of Medicine*, vol. 103, no. 2, pp. S12–S19, Aug. 1997, https://doi.org/10.1016/S0002-9343(97)90022-X.

[8] D. C. Mackey *et al.*, "The Flooring for Injury Prevention (FLIP) Study of compliant flooring for the prevention of fall-related injuries in long-term care: A randomized trial," *PLOS Medicine*, vol. 16, no. 6, Jun. 2019, Art. no. e1002843, https://doi.org/10.1371/journal.pmed.1002843.

[9] I. D. Cameron *et al.*, "Hip protectors: recommendations for conducting clinical trials—an international consensus statement (part II)," *Osteoporosis International*, vol. 21, no. 1, pp. 1–10, Jan. 2010, https://doi.org/10.1007/s00198-009-1055-2.

[10] R. J. Tarbert and W. Singhatat, "Real World Evidence of Wearable Smartbelt for Mitigation of Fall Impact in Older Adult Care," *IEEE Journal of Translational Engineering in Health and Medicine*, vol. 11, pp. 247–251, 2023, https://doi.org/10.1109/JTEHM.2023.3256893.

[11] R. J. Tarbert, J. Zhou, and B. Manor, "Potential Solutions for the Mitigation of Hip Injuries Caused by Falls in Older Adults: A Narrative Review," *The Journals of Gerontology: Series A*, vol. 78, no. 5, pp. 853–860, May 2023, https://doi.org/10.1093/gerona/glac211.

[12] Y. Jeong *et al.*, "Impact Attenuation of the Soft Pads and the Wearable Airbag for the Hip Protection in the Elderly," *International Journal of Precision Engineering and Manufacturing*, vol. 20, no. 2, pp. 273–283, Feb. 2019, https://doi.org/10.1007/s12541-019-00053-9.

[13] T. Tamura, T. Yoshimura, M. Sekine, M. Uchida, and O. Tanaka, "A Wearable Airbag to Prevent Fall Injuries," *IEEE Transactions on Information Technology in Biomedicine*, vol. 13, no. 6, pp. 910–914, Nov. 2009, https://doi.org/10.1109/TITB.2009.2033673.

[14] T. Tamura, T. Yoshimura, M. Sekine, and M. Uchida, "Development of a Wearable Airbag for Preventing Fall Related Injuries," in *Human Centered Design*, vol. 6776, M. Kurosu, Ed. Berlin, Heidelberg: Springer Berlin Heidelberg, 2011, pp. 335–339.

[15] T. Sivaranjani, L. DhiviyaLakshmi, R. Yogaaravinth, J. Srivishnu, M. M. S. Karthick, and A. Praveenkumar, "Fall assessment and its injury prevention using a wearable airbag technology," in *2017 IEEE International Conference on Power, Control, Signals and Instrumentation Engineering (ICPCSI)*, Chennai, Sep. 2017, pp. 2539–2541, https://doi.org/10.1109/ICPCSI.2017.8392175.

[16] G. Shi, C. S. Chan, W. J. Li, K.-S. Leung, Y. Zou, and Y. Jin, "Mobile Human Airbag System for Fall Protection Using MEMS Sensors and Embedded SVM Classifier," *IEEE Sensors Journal*, vol. 9, no. 5, pp. 495–503, May 2009, https://doi.org/10.1109/JSEN.2008.2012212.

[17] S. Ahn *et al.*, "Optimization of a Pre-impact Fall Detection Algorithm and Development of Hip Protection Airbag System," *Sensors and Materials*, vol. 30, no. 8, Aug. 2018, Art. no. 1743, https://doi.org/10.18494/SAM.2018.1876.

[18] S. A. Alshammari and N. S. Albalawi, "Enhancing Healthcare Monitoring: A Deep Learning Approach to Human Activity Recognition using Wearable Sensors," *Engineering, Technology & Applied Science Research*, vol. 14, no. 6, pp. 18843–18848, Dec. 2024, https://doi.org/10.48084/etasr.9255.

[19] S. Sankaran, A. P. Thiyagarajan, A. D. Kannan, K. Karnan, and S. R. Krishnan, "Design and Development of Smart Airbag Suit for Elderly

with Protection and Notification System," in *2021 6th International Conference on Communication and Electronics Systems (ICCES)*, Coimbatre, India, Jul. 2021, pp. 1273–1278, https://doi.org/10.1109/ICCES51350.2021.9488972.

[20] M. Ibrahim, S. Shawish, S. Aldroubi, A. Dawoud, and W. Abdin, "Airbag Protection and Alerting System for Elderly People," *Applied Sciences*, vol. 13, no. 16, Aug. 2023, Art. no. 9354, https://doi.org/10.3390/app13169354.

[21] T. Liu, X. Li, K. Qi, Z. Zhang, Y. Xiao, and S. Guo, "CSAPSO-BPNN-Based Modeling of End Airbag Stiffness of Nursing Transfer Robot," *Electronics*, vol. 13, no. 6, Mar. 2024, Art. no. 1152, https://doi.org/10.3390/electronics13061152.

[22] B. E. Keenan and S. L. Evans, "Biomechanical testing of hip protectors following the Canadian Standards Association express document," *Osteoporosis International*, vol. 30, no. 6, pp. 1205–1214, Jun. 2019, https://doi.org/10.1007/s00198-019-04914-x.

[23] S. N. Robinovitch *et al.*, "Hip protectors: recommendations for biomechanical testing—an international consensus statement (part I)," *Osteoporosis International*, vol. 20, no. 12, pp. 1977–1988, Dec. 2009, https://doi.org/10.1007/s00198-009-1045-4.

[24] D. Bendjaballah, A. Bouchoucha, M. L. Sahli, and J.-C. Gelin, "Numerical analysis of side airbags deployment in out-of-position situations," *International Journal of Mechanical and Materials Engineering*, vol. 12, no. 1, Dec. 2017, Art. no. 12, https://doi.org/10.1186/s40712-016-0070-2.

[25] J. Bai, S. Qi, Y. Xie, M. Yuan, and M. Li, "Ballistic response of an airbag with parallel ribs under spherical projectile impact," *Composite Structures*, vol. 353, Jan. 2025, Art. no. 118734, https://doi.org/10.1016/j.compstruct.2024.118734.

[26] M. Chiba, K. Shimizu, T. Yasui, K. Katayama, A. Yamano, and H. Yutani, "Airbag models for aircraft passenger seats," *International Journal of Crashworthiness*, vol. 26, no. 6, pp. 636–650, Nov. 2021, https://doi.org/10.1080/13588265.2020.1766643.

[27] J. Lee, Y. Choi, C. Jo, and D. Chang, "Design of a prismatic pressure vessel: An engineering solution for non-stiffened-type vessels," *Ocean Engineering*, vol. 142, pp. 639–649, Sep. 2017, https://doi.org/10.1016/j.oceaneng.2017.07.039.

[28] Y. Xiao, T. Liu, C. Meng, Z. Jiao, F. Meng, and S. Guo, "Numerical simulation modeling and kinematic analysis onto double wedge-shaped airbag of nursing appliance," *Scientific Reports*, vol. 13, no. 1, Aug. 2023, Art. no. 14261, https://doi.org/10.1038/s41598-023-41619-y.

[29] E. Arjmand, "Inflatable Hip Protectors," M. Sc. thesis, School of Engineering Science Faculty of Applied Sciences, Simon Fraser University, Burnaby, Canada, 2012.

[30] T. Lee, "Biomechanical effects of shear thickening polymer (STP)-based hip protectors," in *35th Conference of the International Society of Biomechanics in Sports*, Cologne, Germany, Jun. 2017, pp. 14–18.

[31] E. Post, V. Komisar, J. Sims-Gould, A. Korall, F. Feldman, and S. Robinovitch, "Development of a stick-on hip protector: A multiple methods study to improve hip protector design for older adults in the acute care environment," *Journal of Rehabilitation and Assistive Technologies Engineering*, vol. 6, Jan. 2019, Art. no. 2055668319877314, https://doi.org/10.1177/2055668319877314.

[32] W. J. Choi, J. A. Hoffer, and S. N. Robinovitch, "The effect of positioning on the biomechanical performance of soft shell hip protectors," *Journal of Biomechanics*, vol. 43, no. 5, pp. 818–825, Mar. 2010, https://doi.org/10.1016/j.jbiomech.2009.11.023.

[33] S. Hirabayashi, E. Tanaka, Y. Mizuno, H. Nagata, and M. Shibaya, "Development of hip protector with a hole based on biomechanical evaluation," *Transactions of the JSME (in Japanese)*, vol. 80, no. 813, pp. BMS0138–BMS0138, 2014, https://doi.org/10.1299/transjsme.2014bms0138.

[34] A. C. Laing and S. N. Robinovitch, "The Force Attenuation Provided by Hip Protectors Depends on Impact Velocity, Pelvic Size, and Soft Tissue Stiffness," *Journal of Biomechanical Engineering*, vol. 130, no. 6, Dec. 2008, Art. no. 061005, https://doi.org/10.1115/1.2979867.